SUPPORTING INFORMATION

A Thiadiazole-capped Nanoribbon with 18 Linearly-Fused Rings

Diego Cortizo-Lacalle,[a] Cristian Gozalvez, [a] Manuel Melle-Franco,[b] Aurelio Mateo-Alonso*[a,c]

[a]*POLYMAT, University of the Basque Country UPV/EHU, Avenida de Tolosa 72, 20018, Donostia-San Sebastian, Spain.*

[b]*CICECO-Aveiro Institute of Materials, Department of Chemistry, University of Aveiro, 3810-193, Aveiro, Portugal.*

[c]*Ikerbasque, Basque Foundation for Science, E-48011 Bilbao, Spain.*

GENERAL

NR-10-Q and **BTD-NH$_2$** were synthesized according to the literature.[1] Analytical thin layer chromatography (TLC) was carried out using aluminum sheets (20x20 cm) pre-coated with silica gel RP-18W 60 F254 from Merck. Column chromatography was carried out using Silica gel 60 (40-60 µm) from Scharlab. NMR spectra in solution were recorded on a Bruker Avance 400 MHz spectrometer at 298 K using partially deuterated solvents as internal standards. The measurements of High Resolution Mass Spectroscopy (MALDI) were carried by Dr. Javier Calvo in Biomagune in a Ultraflex III (Bruker Daltonics) MALDI-ToF (frequency-tripled (355 nm) Nd:YAG laser) (Matrix: 20 mg/mL dithranol in THF). Absorption and photoluminescence spectra were recorded on a Perkin-Elmer Lambda 950 spectrometer, and a LS55 Perkin-Elmer Fluorescence spectrometer, respectively. Electrochemical measurements were carried out on a Princeton Applied Research Parstat 2273 in a 3-electrode single compartment cell with glassy carbon disc working electrode, a platinum wire counter electrode and a silver wire pseudoreference electrode. All the potential values are reported versus the redox potential of the ferrocene/ferrocenium couple.

1. SYNTHESIS

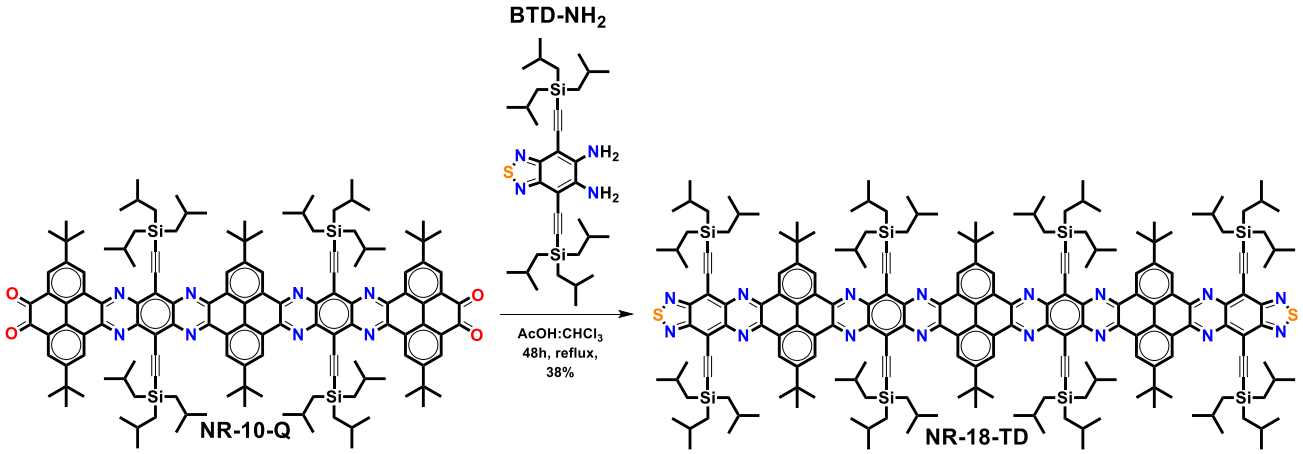

Scheme S1. Synthesis of **NR-18-TD**

NR-10-Q[1] (22 mg, 10.2 µmol, 1.0 eq.) and **BTD-NH$_2$**[1] (25 mg, 40.0 µmol, 4.0 eq.) were dissolved in a chloroform:acetic acid (3:1) mixture. The reaction was refluxed for 48 hours under nitrogen. The mixture was poured in methanol and the precipitate was purified by column chromatography (toluene:chloroform). **NR-18-TD** (13 mg, 38%) was isolated as a dark purple solid. ^{1}H-NMR ($CDCl_3$): δ 10.05 (4H, s), 10.01 (4H, d), 9.94 (4H, d), 2.23-2.13 (24H, m), 1.92 (18H, s), 1.87 (36H, s), 1.20-1.14 (168, m) and 1.03 (24, d). ^{13}C-NMR ($CDCl_3$): δ 155.21, 151.66, 151.55, 145.56, 144.97, 144.79, 142.46, 142.40, 141.83, 129.87, 129.79, 129.50, 127.71, 127.61, 127.56, 127.52, 127.47, 122.13, 114.45, 113.09, 113.00, 102.58, 101.73, 36.16, 36.08, 32.52, 32.35, 29.87, 26.75, 26.71, 25.48, 25.40, and 25.37. HRMS (MALDI, pos.) (m/z): $[M+Ag]^+$ calcd. for $C_{208}H_{282}AgN_{16}S_2Si_8$, 3398.9170; found, 3398.8743.

2. CHARACTERIZATION

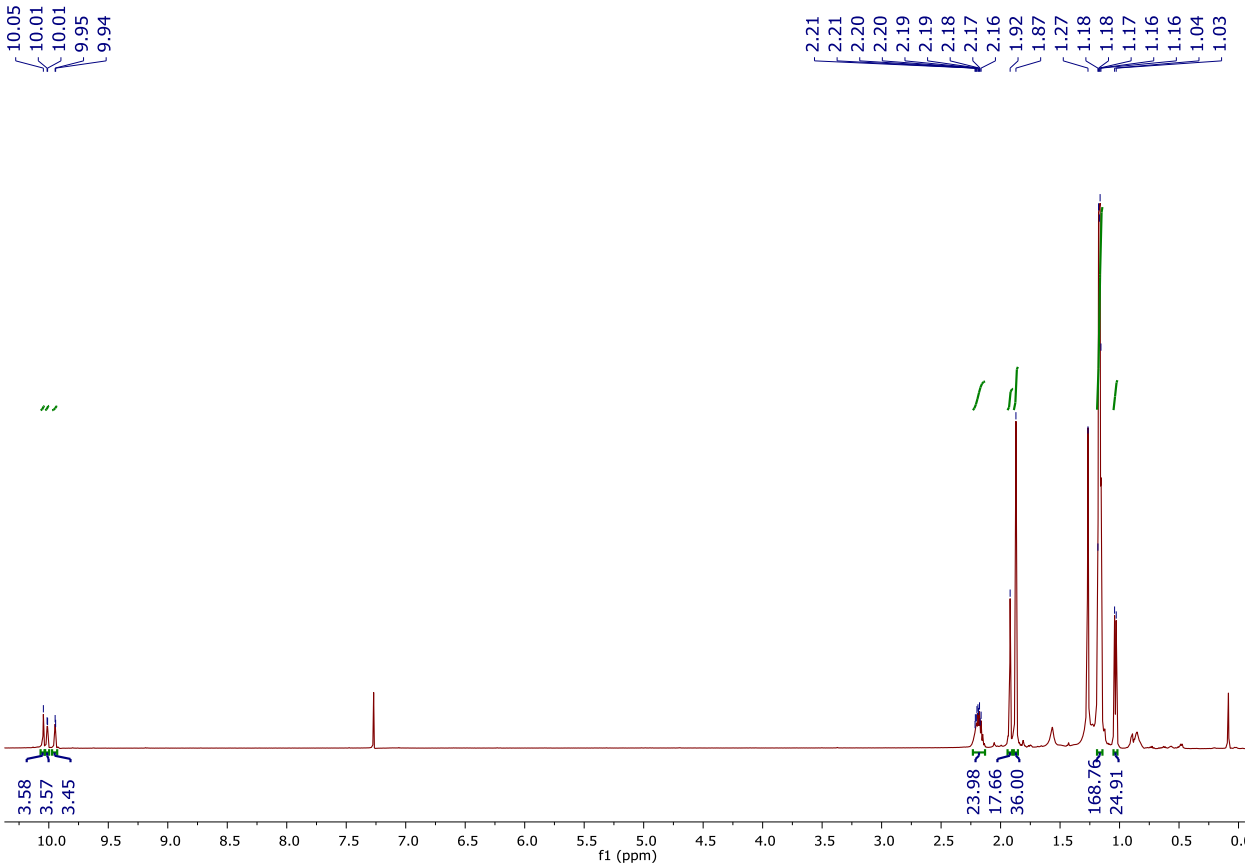

Figure S1. ^{1}H-NMR spectrum of **NR-18-TD** in (400 MHz, $CDCl_3$)

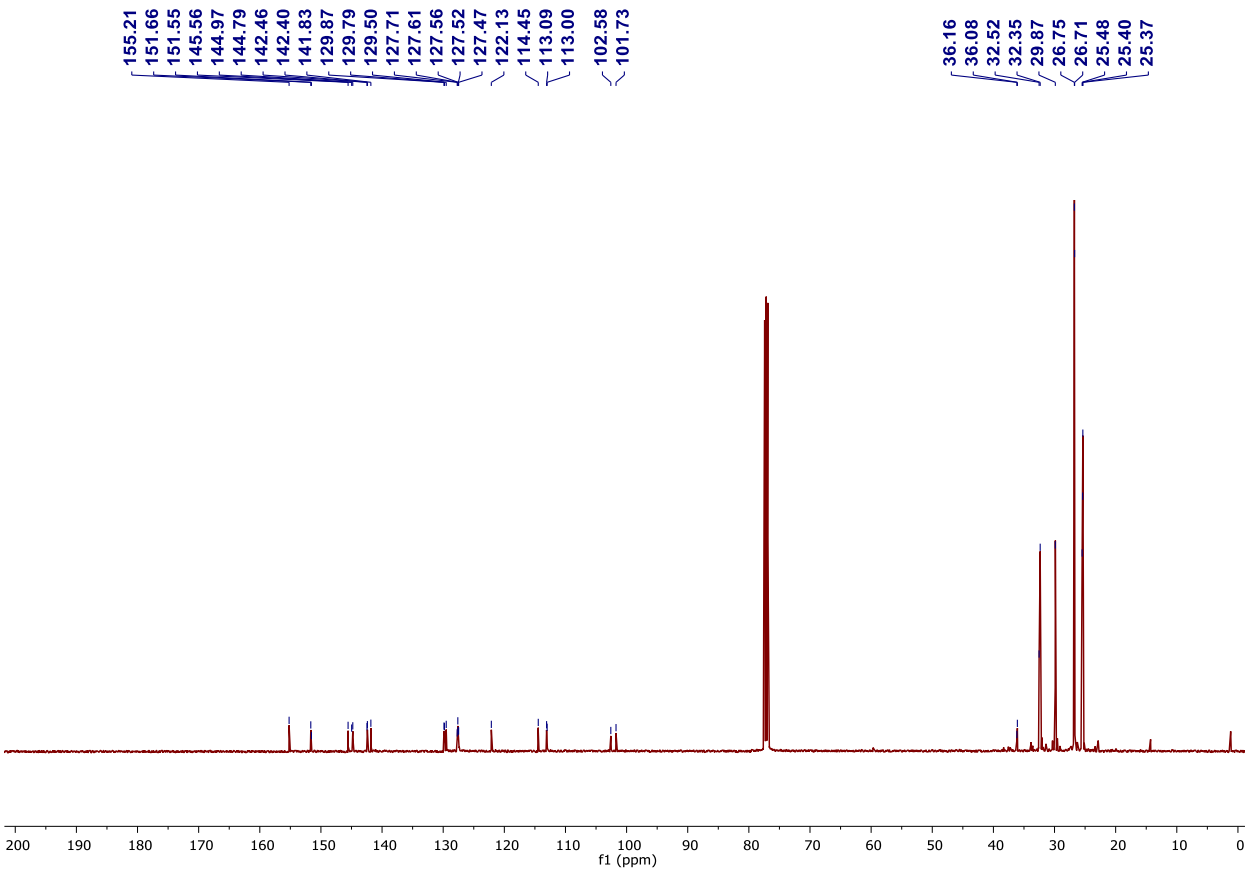

Figure S2. ^{13}C-NMR spectrum of **NR-18-TD** (400 MHz, $CDCl_3$)

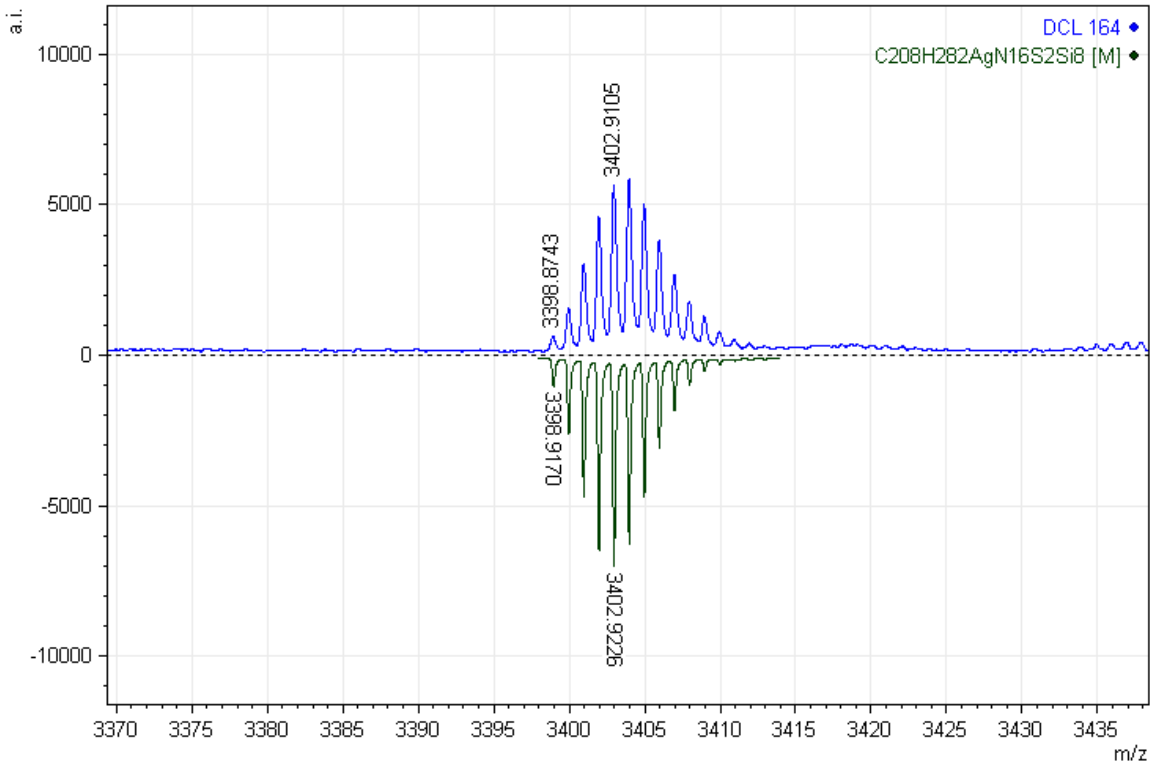

Figure S3. Experimental (top) and calculated (bottom) MALDI-TOF HRMS spectra of **NR-18-TD**.

3. CALCULATIONS

TD-DFT

Table S1. TD-DFT stronger transitions at the B3LYP-6-31g(d,p) level for **NR-18-TD** and **NR-18-TD-H.** The most intense transition is marked in red.

B3LYP 6-31g(d,p)	Trans. #	eV	nm	Osc. Strength	Major contributions
NR-18-TD	1	1.83	677	0.037	H-2->LUMO (25%), H-1->LUMO (50%), HOMO->LUMO (21%)
NR-18-TD	2	1.85	671	0.060	H-2->L+1 (20%), HOMO->L+1 (75%)
NR-18-TD	3	1.89	657	0.120	H-2->L+1 (41%), H-1->L+1 (51%)
NR-18-TD	4	1.89	656	0.128	H-3->LUMO (94%)
NR-18-TD	5	1.92	646	0.231	H-1->L+2 (21%), HOMO->L+2 (59%)
NR-18-TD	17	2.26	550	2.675	H-4->LUMO (23%), H-4->L+1 (14%), H-4->L+2 (46%)
NR-18-TD	23	2.55	486	0.116	H-6->L+2 (44%), H-5->LUMO (21%)
NR-18-TD-H	1	1.97	630	0.019	H-1->L+1 (41%), HOMO->LUMO (51%)
NR-18-TD-H	4	2.05	606	0.165	H-3->L+1 (42%), H-2->LUMO (50%)
NR-18-TD-H	5	2.06	601	0.056	HOMO->L+2 (80%)
NR-18-TD-H	10	2.10	589	0.032	H-3->L+3 (33%), H-2->L+2 (20%), H-1->L+1 (12%), H-1->L+3 (20%), HOMO->LUMO (11%)
NR-18-TD-H	17	2.31	537	2.826	H-4->LUMO (37%), H-4->L+2 (49%)
NR-18-TD-H	19	2.45	505	0.027	H-4->LUMO (49%), H-4->L+2 (43%)
NR-18-TD-H	22	2.64	470	0.357	H-5->L+1 (69%), H-4->LUMO (13%)
NR-18-TD-H	39	2.94	422	0.184	H-6->LUMO (34%), H-6->L+2 (55%)

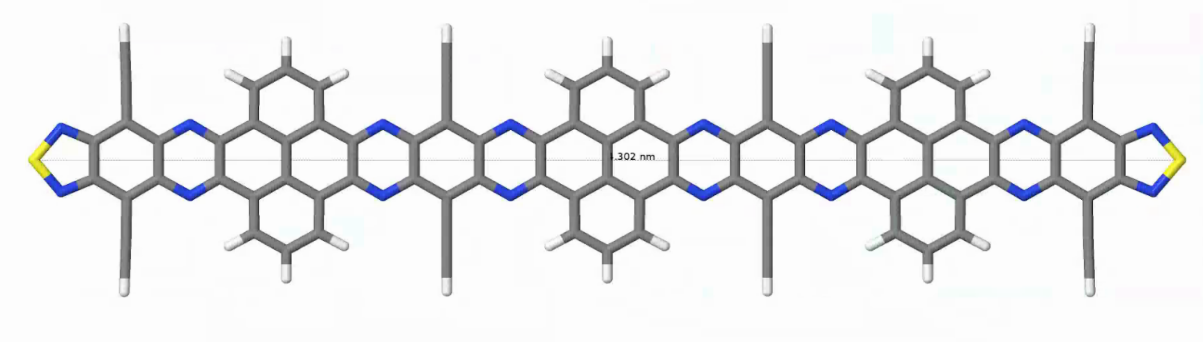

Figure S4. NR-18-TD-H at the B3LYP-6-31g(d,p) level.

Electronic structure

NR-18-TD (516 atoms) is large to compute with DFT while **NR-18-TD-H** (132 atoms) is more manageable computationally. The frontier orbitals energies of **NR-18-TD** computed at the B3LYP-6-31g(d,p) level and the **NR-18-TD-H** at the B3LYP-6-31g(d,p) and at the B3LYP-CH_2Cl_2-6-311+g(2d,p)/B3LYP-6-31g(d,p) level are presented in Table S2. The LUMO value for the aromatic core analogue of **NR-18-TD** is -3.85 eV with the 6-311+g(2d,p) basis set in dichloromethane with the B3LYP Hamiltonian[2] which matches very well the measured value of -3.91 eV.

A comparison with the flat, highly symmetric, **NR-18-TD-H** (Figure S4) molecule allows quantifying the effects on the TD-DFT spectrum due to asymmetries introduced in the molecular structure by the solubilizing groups. The most intense transitions are 1.92 eV and 2.26 eV and 2.05 eV and 2.31 for **NR-18-TD** and **NR-18-TD-H** respectively, Table S1, which can be rationalized by the slightly larger HOMO-LUMO gap of **NR-18-TD-H**, Table S2.

Table S2. Frontier orbitals computed with the B3LYP Hamiltonian with the 6-31g(d,p) basis set in vacuum for **NR-18-TD** and **NR-18-TD** geometries and the 6-311+g(2d,p) basis set in dichloromethane for the aromatic core geometry. All molecular geometries were optimized at the B3LYP-6-31g(d,p) level. The colour code followed is: LUMOs, HOMOs and gaps. **All values in eV.**

B3LYP-6-31g(d,p)																	
NR-18-TD	-1.68	-1.72	-1.78	-1.84	-1.87	-3.26	-3.30	-3.39	-3.41	-5.5	-5.51	-5.52	-5.54	-6.00	-6.19	-6.31	-6.35	2.09
B3LYP-6-31g(d,p)																		
NR-18-TD-H	-1.80	-1.84	-1.90	-1.96	-1.99	-3.37	-3.41	-3.51	-3.51	-5.75	-5.76	-5.77	-5.77	-6.15	-6.36	-6.60	-6.67	2.24
B3LYP-6-311+g(2d,p)-Cl_2CH_2/B3LYP-6-31g(d,p)/B3LYP-6-31g(d,p)																		
NR-18-TD-H	-2.09	-2.11	-2.21	-2.22	-2.29	-3.68	-3.71	-3.85	-3.85	-6.05	-6.07	-6.13	-6.13	-6.32	-6.55	-6.82	-6.83	2.20

Molecular Orbitals

The eigenvalues of both frontier orbitals, HOMO and LUMO, show a quasi degeneration of 4 for **NR-18-TD** (Table S2). Since **NR-18-TD-H** is highly symmetric and flat**,** the comparison with **NR-18-TD** allows us to get some indication of the effect of deformation of the aromatic core due to the solubilizing groups in the electronic properties. The LUMOs for both cases are similar, in contrast the HOMOs show clear asymmetries in **NR-18-TD** (Figure S5), when compared with the highly symmetric case, **NR-18-TD-H** (Figure S6). The effect in the energies is small, and can be approximately quantified with the maximum spread of the eigenvalues in the quasi-degenerate states: ΔE_{LUMO} and ΔE_{HOMO}. ΔE_{LUMO} has a similar value in both cases, ~0.15 eV, in contrast the ΔE_{HOMO} is lower, showing higher degeneracy, yet it presents a larger variation with values of 0.02 eV and 0.04 eV for **NR-18-TD-H** and **NR-18-TD** respectively (Table S2).

LUMO	LUMO+1	LUMO+1	LUMO+3	LUMO+4	LUMO+5
-3.41	-3.39	-3.3	-3.26	-1.87	-1.84

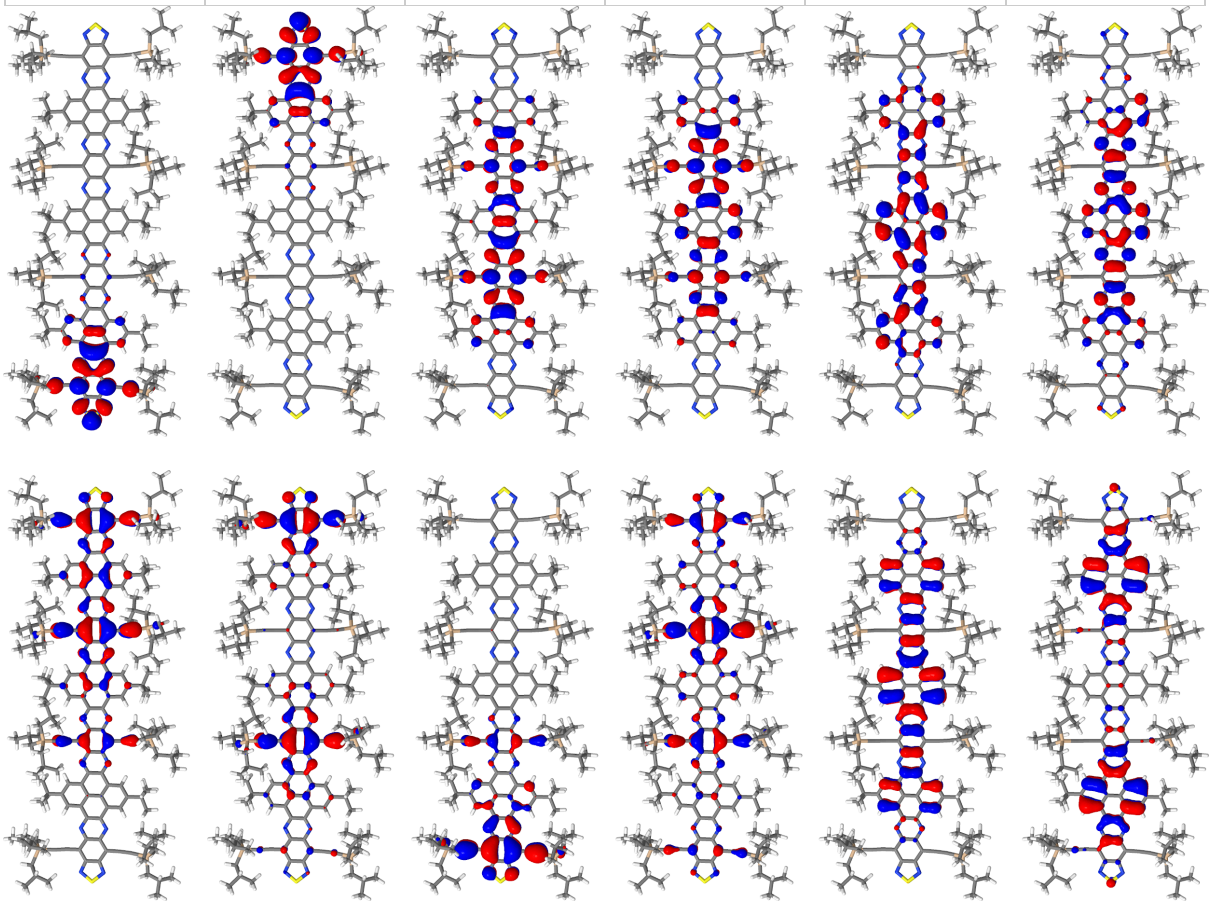

HOMO	HOMO-1	HOMO-2	HOMO-3	HOMO-4	HOMO-5
-5.50	-5.51	-5.52	-5.54	-6.00	-6.19

Figure S5. B3LYP-6-31g(d,p) level frontier orbitals for **NR-18-TD**. The same colour for LUMOs and HOMOs highlights the near degeneracy in energies. **All values in eV.**

LUMO	LUMO+1	LUMO+1	LUMO+3	LUMO+4	LUMO+5
-3.51	-3.51	-3.41	-3.37	-1.99	-1.96

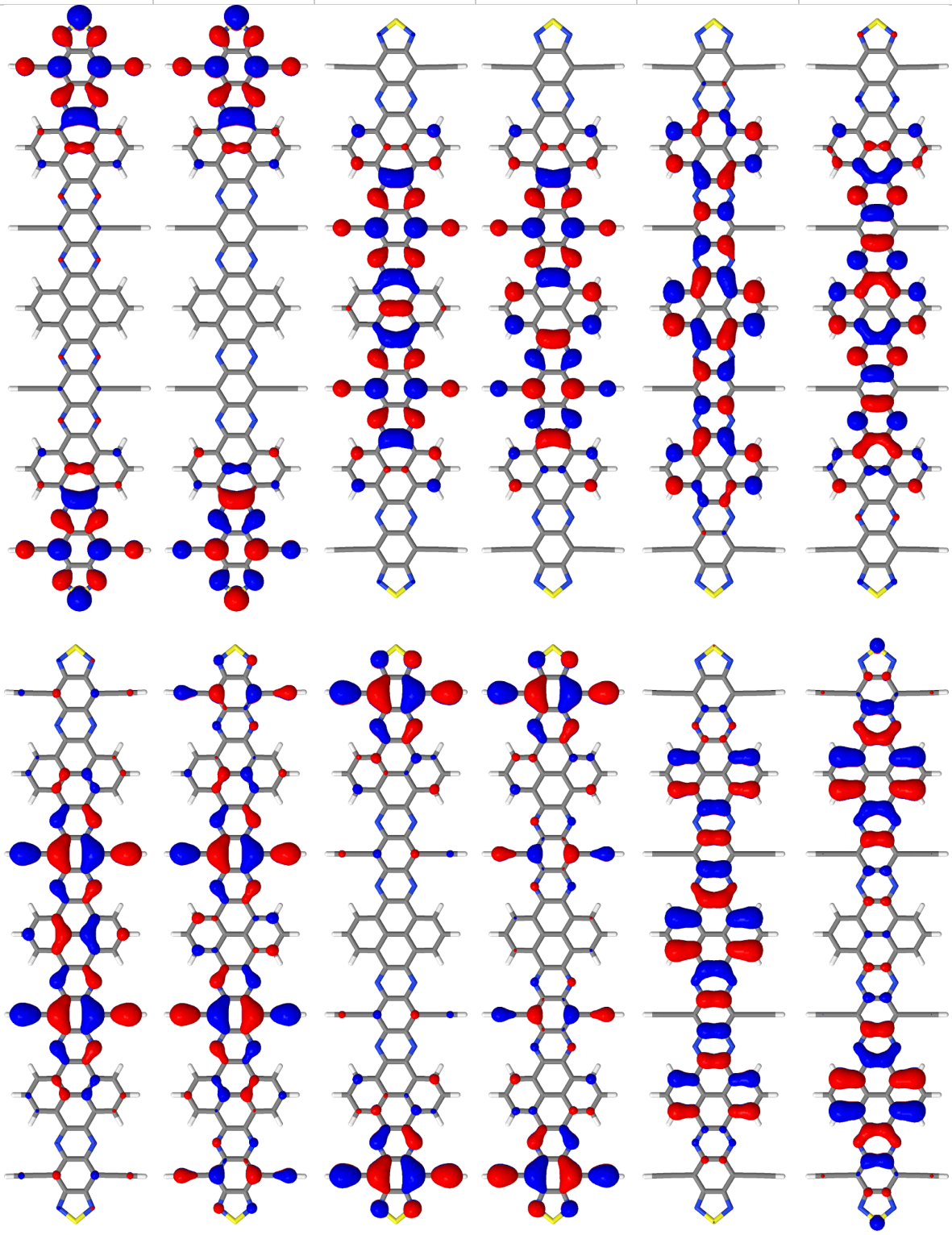

HOMO	HOMO-1	HOMO-2	HOMO-3	HOMO-4	HOMO-5
-5.75	-5.76	-5.77	-5.77	-6.15	-6.36

Figure S6. B3LYP-6-31g(d,p) level frontier orbitals for **NR18-TD-H**. The same colour for LUMOs and HOMOs highlights the orbitals with near degeneracy in energies. **All values in eV.**

4. PREPARATION AND MEASUREMENT OF DEVICES

Commercially available interdigital Au electrodes (15x15 mm^2) from Fraunhofer IPMS were used. High doped *n*-type silicon was employed as gate electrode. A 30 nm Au electrode with a 10 nm high work function adhesion layer (ITO) (structured by lift-off technique) was patterned as source and drain electrodes respectively on the gate dielectric of 230-nm thermal-oxidized SiO_2. First, the electrodes were cleaned one by one by ultrasonication with electronic grade acetone and *iso*propanol and dried under compressed N_2. Then, the electrodes were treated with oxygen plasma for 15 minutes. To form self-assembled monolayers (SAMs) of octadecyltrichlorosilane (OTS) on the SiO_2 surface, the substrates were dipped into a solution of OTs (4 mM) in toluene and heated at 50 ^oC during 30 minutes. The modified electrodes were subsequently washed with chloroform and dried for 1 hour at 80 ^oC. Finally, the substrates were cleaned again with electronic grade acetone and *iso*-propanol and dried with N_2.

On the one hand, films of **NR-18-TD** were deposited spin-coating a solution of $CHCl_3$ (4 mg/mL) and toluene (4 mg/mL), both at 1000 rpm with an acceleration of 1000 rpm/s^2 during 20 s. On the other hand films of **NR-18-TD** were deposited drop-casting a solution of toluene (4 mg/mL). The electrical characterization of the devices was carried out with a Keithley 2636B semiconductor analyzer system, which connected to a probe-station under nitrogen at room temperature.
The mobility of each electrode was calculated in the saturation regime using Equation 1:

$$I_{DS,sat}=\frac{CiW}{2L}\ \mu_{FE}\left(V_{GS}-V_T\right) \quad \text{Equation 1}$$

Where μ_{FE} is the field-effect mobility, C_i is the capacitance per unit area of the dielectric layer, L is the channel length, W is the channel width, V_T is the threshold voltage and V_{GS} is the gate-source bias.

Table S3. Performance and the parameters obtained from the measurement of the Organic Thin Film Transistors (OTFTs) of **NR-18-TD**. All samples were measured under inert conditions. a) Average of electron mobility of the different channel width (W) and length (L) of each device performed.

Method	Solvent	Anneling (^oC)	μ_e [a]	$\mu_{e,max}$	V_{th}	I_{on}/I_{off}
Spin-coating	$CHCl_3$	80	$5.5x10^{-6}$	$9.4\ x10^{-6}$	35	$1.5x10^3$
Spin-coating	$CHCl_3$	160	$3.9x10^{-5}$	$6.6x10^{-5}$	47	$1.2x10^3$
Spin-coating	Toluene	80	$1.8x10^{-5}$	$4.4x10^{-5}$	43	$7.6x10^2$
Spin-coating	Toluene	160	$5.2x10^{-5}$	$1.0x10^{-4}$	47	$1.3x10^3$
Drop-casting	Toluene	80	$1.7x10^{-5}$	$3.4x10^{-5}$	37	$1.3x10^3$
Drop-casting	Toluene	160	$4.5x10^{-5}$	$1.4x10^{-4}$	31	$8.9x10^1$

5. REFERENCES

1. D. Cortizo-Lacalle, J. P. Mora-Fuentes, K. Strutyński, A. Saeki, M. Melle-Franco and A. Mateo-Alonso, *Angew. Chem. Int. Ed.*, 2018, **57**, 703-708.
2. A. B. Marco, C. Gozalvez, M. Olano, X. Sun, A. Atxabal, M. Melle-Franco, L. E. Hueso and A. Mateo-Alonso, *Phys. Chem. Chem. Phys.*, 2016, **18**, 11616-11619.